Quantitative Aeroelastic Stability Prediction of Wings Exhibiting Nonlinear Restoring Forces

Aykut Tamer

Department of Mechanical Engineering, University of Bath, Bath / UK

Abstract

In engineering practice, eigen-solution is used to assess the stability of linear dynamical systems. However, the linearity assumption in dynamical systems sometimes implies simplifications, particularly when strong nonlinearities exist. In this case, eigen-analysis requires linerisation of the problem and hence fails to provide a direct stability estimation. For this reason, a more reliable tool should be implemented to predict nonlinear phenomena such as chaos or limit cycle oscillations. One method to overcome this difficulty is the Lyapunov Characteristic Exponents (LCEs), which provides quantitative indications of the stability characteristics of dynamical systems governed by nonlinear time-dependent differential equations. Stability prediction using Lyapunov Characteristic Exponents is compatible with the eigen-solution when the problem is linear. Moreover, LCE estimations do not need a steady or equilibrium solution and they can be calculated as the system response evolves in time. Hence, they provide a generalization of traditional stability analysis using eigenvalues. These properties of Lyapunov Exponents are very useful in aeroelastic problems possessing nonlinear characteristics, which may significantly alter the aeroelastic characteristics, and result in chaotic and limit cycle behaviour. A very common nonlinearity in flexible systems is the nonlinear restoring force such as cubic stiffness, which would substantially benefit from using LCEs in stability assessment. This work presents the quantitative evaluation of aeroelastic stability indicators in the presence of nonlinear restoring force. The method is demonstrated on a two-dimensional aeroelastic problem by comparing the system behaviour and estimated Lyapunov Exponents.

1. Introduction

Linear system aeroelasticity is extensively studied in literature as presented in Ref. [1]. Stability indicators of linear, time-invariant (LTI) problems are evaluated by conducting eigen-analysis and extracting the real part of the eigenvalues of its state space matrix, which is a constant matrix by definition. This solution provides a spectrum of the system's orthogonal behaviour, namely modes. Stability evaluation is more complex if the linear problem is time-dependent, i.e. the elements in the state space matrix explicitly depend on time. A specific time-dependent problem is when these matrices are periodic. In this case, confirming to Floquet method, the stability properties of the system can be evaluated using eigen-solution. However, this time the real parts of the logarithm of the eigenvalues of the state transition matrix separated by the system's period (monodromy matrix) are defined as the stability indicators.

Nonlinearities always arise in aeroelastic systems, which sometimes become non-negligible. Typical sources of the nonlinearities are structure, aerodynamics, joints (bolts, fasteners etc), friction and control systems. When nonlinearities dominate, unique phenomena arise, which cannot be predicted using linear stability theory. Among them, self-sustained oscillations, also referred to as limit cycle oscillations (LCO), occur without needing external input [2]. Additionally, more complex responses may exist, such as chaotic motion [3]. Many experiments and observations on aeroelasticity problems mention phenomena of nonlinear origin. Therefore, understanding and analyzing nonlinearities in aeroelasticity is crucial for safer, more efficient, and advanced designs [4]. Nonlinear aeroelastic problems can be analyzed using theoretical and numerical methods such as wind tunnel experiments, nonlinear simulations or conducting flight tests [5].

For nonlinear, time-invariant dynamical systems, the eigenvalues and eigenvectors of the linear model computed at points on the phase plane related to a steady-state solution provide localized information on the stability in the vicinity of those points. If enough points are considered and a sufficiently large phase plane is constructed, it is possible to reach a geometric and qualitative understanding of a system's stability. However, these methods are not as practical and useful as eigen-solution, which provides a spectrum and stability characteristics of each branch (corresponding to modes in a linear system). Especially, for systems having higher degrees of freedom, geometric identification is not straightforward; thus, a quantitative method would be more useful.

A method, which gives insight into the stability characteristics of the system and, simultaneously, provides a practical means for its analysis would be very useful in nonlinear time-dependent system dynamics. Such a method is expected to: i) work without a special reference or steady-state solution (i.e. equilibrium point or a stable orbit); and ii) provide indications about the existence of nonlinear characteristics (such as an attractor, a periodic orbit or a higher-order solution), during computation of the system's evolution in time. Lyapunov Characteristic Exponents (LCEs in short) are indicators of the stability characteristics of the solutions of differential equations [6, 7]. In other words, LCEs identify the spectrum of the corresponding initial value problem [8]. LCEs can be applied to a wide range of dynamical systems, including those governed by nonlinear time-dependent differential equations.

The use of LCEs is suggested as a technique for predicting the stability of nonlinear aeroelastic problems [5]. Mostly, the LCEs estimates based on time series were studied in the literature [9]. Ref. [10] presented the aeroelastic response of a wing section with nonlinearities of structural origin; where LCO and chaotic response were identified and compared with estimates of Lyapunov Exponents based on time series analysis. In Ref. [11], chaos and chaotic transients were shown to exist in aeroelastic systems. In another work, nonlinearities originated from aerodynamics and physical parameters were investigated for an airfoil under supersonic flow by Ref. [12], where bifurcations were identified using First Lyapunov Quantity. While the above literature estimate LCEs from time series, the LCE stability indication working directly on system differential equation rather than calculating them using time series, was recently introduced into rotorcraft stability assessment in Ref. [13], where accurate predictions of nonlinear phenomena were observed. In addition to research on LCEs, their analytical sensitivity was also investigated in Ref. [14]. The extension of the LCE approach to multi-body dynamics is under investigation and would be a promising contribution to the stability assessment of problems formulated using differential-algebraic equations [15–17].

With the improved nonlinear analysis tools, the nonlinearities can be tolerated and even intentionally included in the design [18]. Use of as the use of extremely flexible wings [19] is an example where nonlinearities arise. In particular, cubic restoring forces are commonly encountered and can induce a substantial effect on the system stability, which is characterized by the presence of a quadratic term in the stiffness coefficient [4]. In the literature, this problem has been investigated numerically and experimentally to determine the effects of the cubic spring on the aeroelastic stability of airfoils. Depending on the characteristics of the cubic spring, namely a soft or a hard one, the flutter characteristics of the system can change significantly and depend on the initial conditions [20]. It is also observed that the limit cycle oscillations is a common consequence of a cubic restoring moment (See for example Refs. [10, 21–23]). Therefore, quantitative means of estimations of stability indicators could be useful in the design phases of aircraft when analyzing possible outcomes due to cubic stiffness effects.

An aeroelastic system needs to operate in a stable region without exhibiting chaotic or divergent behaviour. This work presents quantitative stability estimation of aeroelastic problems involving cubic restoring force nonlinearity. LCEs are implemented along with the differential equations governing the system. The LCEs and simulations have been used to show that the nonlinear term provides stability to the aeroelastic system examined and, the system would be unstable without it. In other words, the system's state transition matrix is directly used rather than first simulating the system and later working on time series. LCE estimation is obtained using the discrete QR method along with simulating the problem in time.

This work is organized as follows. The next section discussed the stability problem of nonlinear systems and Lyapunov characteristic exponents including practical means of estimating LCEs. Then, a two-degree-of-freedom nonlinear aeroelastic problem with unsteady aerodynamics was explained. The stability of the aeroelastic model to perturbations was calculated using LCEs. The stability indications of LCEs were verified by comparing them with the evolution of the system response to initial perturbations.

2. Method

This section presents the nonlinear time-dependent problems and introduces Lyapunov Characteristic Exponents for predicting and quantifying their stability characteristics. In addition, the numerical procedure for their practical estimation of LCEs was also presented with a set of criteria that would help to interpret the LCEs of a dynamical system.

2.1. Stability of dynamical systems

Engineering systems that are governed by differential equations of the form:

$$\dot{\mathbf{x}} = f(\mathbf{x}, t) \quad \text{for} \quad \mathbf{x}(t_0) = \mathbf{x}_0, \tag{2.1}$$

often arise in engineering practice. The linear time-variant problem is one of the special cases:

$$\mathbf{f}(x, t) = \mathbf{A}(t)\mathbf{x}(t),$$

where the state space matrix is not constant but changes with time. In many other cases, the state space matrix is constant, hence the system is time-invariant (LTI). In other words:

$$\dot{\mathbf{x}} = \mathbf{A}\mathbf{x}$$

with $\mathbf{A}$ being constant in time.

The stability of LTI problems is determined by calculating the eigenvalues of constant state space matrix $\mathbf{A}$, also referred to as the system's spectrum. Stability is identified by the real part of the eigenvalues: stable if negative, marginally stable if zero, and unstable if positive.

Stability prediction is more complicated if the system is linear time-dependent. The most common time dependence is periodicity. If the system is linear time periodic (LTP), the state space matrix A has periodic coefficients and repeats itself at time steps separated by period T:

$$\dot{\mathbf{x}} = A(t)\mathbf{x} \quad \text{where} \quad \mathbf{A}(t+T) = \mathbf{A}(t).$$

In this case, LTP system stability is evaluated using the real part of the logarithm of the eigenvalues of the monodromy matrix $\mathbf{H}$. The monodromy matrix $\mathbf{H}$ is defined as the state transition matrix $\mathbf{Y}$ between two temporal states separated by one period (T):

$$\mathbf{H} = \mathbf{Y}(T,0)$$

and the state transition matrix $\mathbf{Y}$ is the solution to the problem:

$$\dot{\mathbf{T}} = \mathbf{A}(t)\mathbf{Y}, \quad \mathbf{Y}(0) = \mathbf{I}$$

where $\mathbf{I}$ is the identity matrix, which denotes an initial perturbation with unit magnitude along all the degrees of freedom of the system. Both linearity and periodicity could mean simplifications to the real behaviour, which is represented by the most general form in Eq. (2.1). The stability prediction in the most general sense (nonlinear and time-dependent) cannot be directly predicted using eigen-analysis, which requires simplifications or assumptions on the real system behaviour.

2.2. Lyapunov characteristic exponents

The formulation of stability is less intuitive for nonlinear time-dependent dynamical systems. Yet, stability has the same interpretation, which can be defined as the decaying rate of the response amplitude after a perturbation. Stability is indicated by the solution of eigen-analysis for linear systems as explained in the previous section. For non-linear time-variant systems, the Lyapunov Exponents can be considered as an extension of linear eigen-analysis to nonlinear time-dependent systems and LCEs provide a more reliable and general indicator of suitability. Consider the problem in Eq. (2.1), with state vector $\mathbf{x}$, and time t, and the nonlinear time-dependent function $\mathbf{f}(x,t)$ with a solution $\mathbf{x}(t)$ for prescribed initial conditions $\mathbf{x}(t_0) = \mathbf{x}_0$. The Lyapunov Characteristic Exponents (λ_i) of this system are defined as:

$$\lambda_i = \lim_{t \to \infty} \frac{1}{t} \log \frac{||_i\mathbf{x}(t)||}{||_i\mathbf{x}(t_0)||},$$

In the above equation, $_i\mathbf{x}(t)$ is geometrically defined as the solution that describes the exponential evolution of the $i-th$ axis of the ellipsoid that grows from an initially infinitesimal n-sphere (representing unit perturbations along each axis) according to the Jacobian $\mathbf{f}_{/\mathbf{x}}$ tangent to $\mathbf{f}$ along the fiducial trajectory $\mathbf{x}(t)$. That is, $_i\mathbf{x}(t)$ is the solution to the linear, time-dependent problem $_i\dot{\mathbf{x}}(t) = \mathbf{f}_{/\mathbf{x}}(\mathbf{x},t)_i\mathbf{x}(t)$, with $_i\mathbf{x}(t_0) =_i \mathbf{x}_0$. This is graphically represented in Figure 2.1.

In engineering-related terms, LCEs provide a measure of the rate of growth of perturbed solutions. The LCE formula involves an unbounded limit for time t approaches infinity. As a result, in practice, the LCEs can only be numerically calculated for a sufficiently large value of t such that the calculations are truncated for converged LCEs. For this reason, the LCEs usually, except for very simple problems, mean that they are numerically estimated for a large enough value of t, where the LCEs converge to a value.
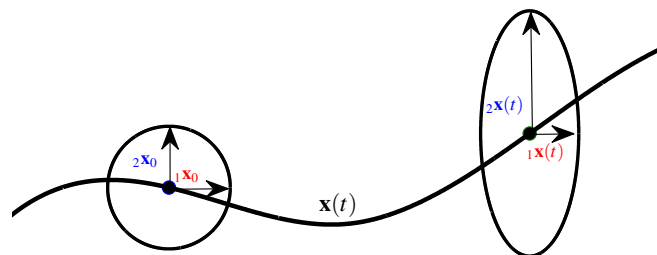

Figure 2.1: Evolution of a perturbation of a solution of a differential equation.

2.3. Numerical estimation of LCEs

Practical calculation of LCEs faces the difficulty of operating on matrices with coefficients quickly diverging (instability) or converging to zero (exponential stability). To solve this problem, several approaches were developed. Continuous formulations for the prediction of the LCEs can be achieved using singular value decomposition (SVD) or through QR decomposition [24]. An alternative technique is the Schur decomposition, which could provide better results in the case of multiple LCEs [25], which is especially advantageous when LCEs appear in multiples. Discrete methods are more practical than continuous ones as they can be more computationally feasible and can be applied to more complex problems in engineering. Among the available methods of LCE estimation, a famous one is the Discrete QR Method. It is derived from incrementally calculating the QR decomposition applied on the state transition matrix at every time step of numerical integration. For its practicality, the discrete QR approach is selected as the LCE computation method in this study and explained hereafter.

2.4. Discrete QR method

The discrete QR method computes LCEs by updating the LCEs estimates with the diagonal elements of the upper-triangular matrix R gathered from incremental QR decompositions of the state transition matrix between two successive time steps. Considering the previously defined state transition matrix $\mathbf{Y}(t,t_j)$ from time t_{j-1} to time t, the state transition matrix is defined as $\mathbf{Y}_j = \mathbf{Y}(t,t_j)$. Then, compute

the QR decomposition of $\mathbf{Y}_j\mathbf{Q}_{j-1}$, starting from $\mathbf{Q}_0 = \mathbf{I}$ (representing a perturbation on each system degree of freedom), which implies $\mathbf{Q}_j\mathbf{R}_j = \mathbf{Y}_j\mathbf{Q}_{j-1}$. After defining $\mathbf{R}_{\Pi j} = \Pi_{k=0}^j \mathbf{R}_{j-k}$, ($\Pi$ is the product operator), it can be shown that:

$$\mathbf{Y}_j\mathbf{Q}_{j-1}\mathbf{R}_{\Pi_{j-1}} = \mathbf{Q}_j\mathbf{R}_{\Pi_j}.$$

Then, $\mathbf{Y}_j\mathbf{Q}_{j-1}\mathbf{R}_{\Pi_{j-1}}$ can be utilized to form $\mathbf{R}_j$ by implementing incremental QR decompositions of $\mathbf{Y}_j\mathbf{Q}_{j-1}$. Thanks to the limited contraction/expansion due to the small time step, matrices do not have rapidly diverging or vanishing elements. The LCEs are then calculated using $\mathbf{R}_{Pi_j}$ as:

$$\lambda_i \quad = \lim_{j\to\infty} \frac{1}{t_j} \log r_{ii}(t_j), \tag{2.2}$$

where $r_{ii}(t_j)$ represents the diagonal elements of $\mathbf{R}_j = \mathbf{R}_{\Pi_j}$ matrix. Eq. (2.2) can further be arranged by considering that the logarithm involving multiplication can be converted to summation, which leads to:

$$\lambda_i \quad = \lim_{j\to\infty} \frac{1}{t_j} \sum_{k=0}^j \log(r_{k_{ii}}).$$

2.5. Quantitative stability assessment

In practice, the obtained LCEs are indicators of the stability properties of a dynamical system. If the system is linear, then the LCEs are equivalent to the real part of the eigenvalues of the state-space matrix. In the case of the nonlinear system, the following criteria could be used to interpret the LCEs:

- The solution is exponentially stable if all LCEs are negative.
- If at least one of the LCEs is positive, the solution is unstable or leads to a chaotic attractor.
- When the largest LCE is zero, or the largest LCEs are zero, a limit cycle oscillation is expected; i.e., the solution neither expands nor contracts.

3. Aeroelastic Problem

This section presents a two-degree-of-freedom aeroelastic problem and its quantitative stability assessment to demonstrate the LCE approach in stability assessment. The example is related to a cubic representation of the restoring pitch moment of an airfoil, which can be seen as a simplification of a wing or control surface.

3.1. Flutter of aircraft wings

Aeroelasticity deals with the interaction of aerodynamic forces and elastic deformations and investigates the influences of wing deformations on airloads [26]. The major problems are divergence and flutter. While the former is static unstable feedback between the deformations and loads; the latter also involves inertial forces and results in an unstable condition where the streamlined body extracts energy from the airflow [27].

A typical aeroelastic system starts with total positive damping coming from the structure aerodynamics at low airspeed, meaning that the system stabilizes itself after perturbations. The damping increases up to a maximum, after which it starts reducing due to aeroelastic interactions. As the flight speed is further increased damping becomes zero and eventually negative, which indicates that the structure extracts energy from the flow. The result is an unstable system where the perturbations grow in amplitude with the extracted energy. The flutter analysis is therefore required to determine at which airspeed the damping becomes zero (onset of instability) and then leave a safety margin below that speed to assess the maximum safe flight speed.

3.2. Model

The most proper method to analyze flutter is to build the full finite element model with unsteady aerodynamics. Having said this, the first bending and first torsion modes of the wing couple interact with unsteady aerodynamics in the most common flutter problem. For this reason, two degrees of freedom models reduced from detailed models or identified through experiments are frequently used in flutter calculations to gain more insight into the physics of the problem during preliminary design and/or reduce computation time [28]. With the same motivation, this work follows the classical two-degree of freedom aeroelastic wing model representing the wing plunging and pitching motions coupled with unsteady aerodynamics.

Figure 3.1 presents the cross-section of a wind-tunnel model of a wing with chord length $2b$. The pitch (α), and plunge (w) degrees of freedom are supported by springs and dampers (dampers not shown for clarity but are connected exactly at the same points where springs are attached). The positions of the elastic axis a and the centre of gravity x_α are normalized by half-chord length b. The mass of the wing is represented by m_w, and the total mass including wing and support is denoted by m_T. S and I are the first and second moments of inertia with respect to the rotation axis. In the equations, subscripts α and w indicate the parameters corresponding to that motion.

3.3. Equations of motion

The mathematical representation of the model presented in Figure 3.1 was obtained from Ref. [29], with parameters reported in Table 3.1. The model is linear except for the pitch spring which has cubic restoring force. For this reason, the problem is separated into linear state space form and nonlinear forcing:

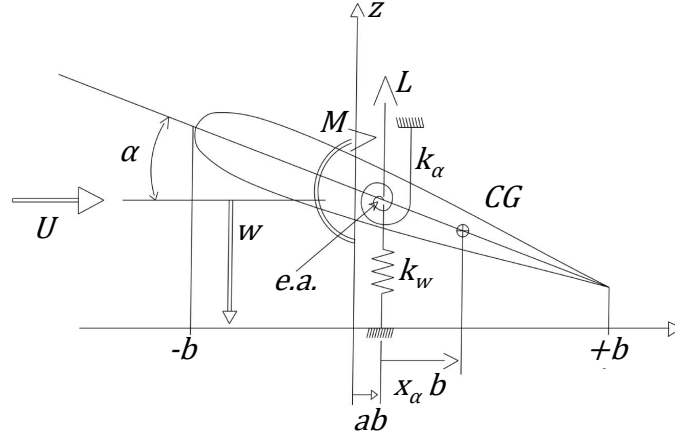$$\mathbf{M}\ddot{\mathbf{x}} + \mathbf{C}\dot{\mathbf{x}} + \mathbf{K}\mathbf{x} = \mathbf{f}_{nl}$$

Figure 3.1: Two degrees of freedom aeroelastic wing.

Variable Description	Value
Span, s	0.6 m
Semi-chord, b	0.0325 m
Position of elastic axis normalized by semi-chord, a	-0.5
Centre of gravity normalized by semi-chard, x_α	0.5
Air density, ρ	1.225 kg/ m^3
Mass of the wing, m_W	1.0662 kg
Mass of wing and supports, m_T	3.836 kg
Moment of inertia about elastic axis, I_α	4067.5 N m s rad^{-1}
Pitch and plunge damping coefficients, c_α, c_h	0.0115,0.011 kg m s^{-2}
Stiffness in pitch and plunge, k_α, k_h	0.942,0.895 N m^{-1}
Stiffness constants of nonlinear damper, $k_{\alpha1}, k_{\alpha2}$	3.95, 107.0 N m

Table 3.1: Parameters of aeroelastic model [22]

In the above equation, $\mathbf{x} = [w \ \ \alpha \ \ \xi]^T$ is the state vector for plunging w, pitching α and augmented state ξ. $\mathbf{f}_{nl}$ is the nonlinear forcing due to cubic spring force. and $\mathbf{K}$, $\mathbf{C}$, and $\mathbf{M}$ are linear stiffness, damping, and mass matrices including unsteady aerodynamics. For the linear part, the mass, stiffness and damping matrices are given as:

$$\mathbf{M} = \mathbf{M}_{structural} + \mathbf{M}_{aero} = \begin{bmatrix} m_T & m_w x_\alpha b & 0 \\ m_w x_\alpha b & I_\alpha & 0 \\ 0 & 0 & 0 \end{bmatrix} + \begin{bmatrix} \pi\rho b^2 & -a\pi\rho b^3 & 0 \\ -a\pi\rho b^3 & \pi(\frac{1}{8}+a^2)\rho b^4 & 0 \\ 0 & 0 & 1 \end{bmatrix}$$

$$\mathbf{C} = \mathbf{C}_{structural} + \mathbf{C}_{aero} = \begin{bmatrix} c_h & 0 & 0 \\ 0 & c_\alpha & 0 \\ 0 & 0 & 0 \end{bmatrix} + \begin{bmatrix} 2\pi\rho bc_5U & (1+c_5)(1-2a)\pi\rho b^2U & 2\pi\rho U^2 bc_6 \\ -2\pi(a+\frac{1}{2})\rho b^2 c_5U & (\frac{1}{2}-a)(1-c_5(1+2a))\pi\rho b^3U & -2\pi\rho b^2U^2(a+\frac{1}{2})c_6 \\ \frac{-1}{b} & a-\frac{1}{2} & (c_2+c_4)\frac{U}{b} \end{bmatrix}$$

$$\mathbf{K} = \mathbf{K}_{structural} + \mathbf{K}_{aero} = \begin{bmatrix} k_h & 0 & 0 \\ 0 & k_{\alpha0} & 0 \\ 0 & 0 & 0 \end{bmatrix} + \begin{bmatrix} 0 & 2\pi\rho bc_5U^2 & 2\pi\rho U^3 c_2 c_4 (c_1+c_3) \\ 0 & -2\pi(\frac{1}{2}+a)\rho c_5 b^2U^2 & -2\pi\rho bU^2(a+\frac{1}{2})c_2 c_4(c_1+c_3) \\ 0 & -\frac{U}{b} & c_2 c_4 \frac{U^2}{b^2} \end{bmatrix}$$

where the subscripts refer to the structural and aerodynamic contribution to the matrices. The structural matrices are symmetric as expected, but the aerodynamic terms spoil the symmetry in the matrices.

It should be emphasized here that the system has two degrees of freedom, but an augmented state (ξ) was added based on Wagner's function for arbitrary (i.e. not only valid for simple harmonic motion) airfoil motion. The use of the formulation for arbitrary motion allows us to identify damping at any flight speed. Since this work aims to provide a generalized method, arbitrary motion is more suitable than the harmonic motion formulation which is only valid when damping is zero and hence invalid except for flutter speed [1]. The constants are given as $c_0 = 1.0$, $c_1 = 0.165$, $c_2 = 0.0455$, $c_3 = 0.335$, $c_4 = 0.3$, and the dependent variables $c_5 = c_0 - c_1 - c_3$, $c_6 = c_1 c_2 + c_3 c_4$.

The cubic restoring force is added to the pitching motion in this example, which has a stiffness coefficient of $k(\alpha) = k_{\alpha0} + k_{\alpha1}\alpha + k_{\alpha2}\alpha^2$. The linear stiffness term $k_{\alpha0}$ is already included in the linear part function, so the nonlinear term can be stated as:

$$\mathbf{f}_{nl} = \begin{bmatrix} 0 & (k_{\alpha1}\alpha + k_{\alpha2}\alpha^2)\alpha & 0 \end{bmatrix}^T$$

The above matrices can be blended into a state space form as:

$$\dot{\mathbf{x}} = \mathbf{A}\mathbf{x} + \mathbf{g}$$

where

$$\mathbf{x}_s = [\mathbf{x} \quad \dot{\mathbf{x}}], \quad \mathbf{A} = \begin{bmatrix} \mathbf{0} & \mathbf{I} \\ -\mathbf{M}^{-1}\mathbf{K} & -\mathbf{M}^{-1}\mathbf{C} \end{bmatrix}, \quad \mathbf{g} = \begin{bmatrix} \mathbf{0} & -\mathbf{M}^{-1}\mathbf{f}_{nl} \end{bmatrix}^T. \tag{3.2}$$

The above equation can now be solved numerically for the given initial conditions and LCEs can be calculated as the simulation continues. Note that when $\mathbf{g} = \mathbf{0}$, the system is linear. In the nonlinear form, the presence of α on the right-hand side spoils the linearity and dominates the response depending on the value of spring constants and α.

4. Results

The linear flutter speed can be calculated by tracking the real part of the eigenvalues of linear state space matrix A of Eq. (3.2) as flight speed is changed and by omitting the nonlinearities in the pitch stiffness. By doing so, the flutter speed was numerically found to be $U_f = 10.90$ m s^{-1} by using the speed-damping (V-g) curve for the lowest damping (λ_1: real part of the largest eigenvalue) as shown in Figure 4.1. At speeds below the flutter speed, the wing is stable. On the contrary, the wind is unstable at flight speeds higher than the flutter speed. The flutter speed is in agreement with the results of Ref. [22].
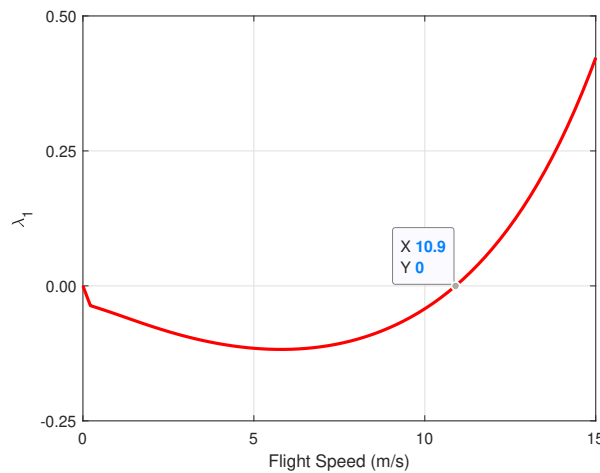

Figure 4.1: Linear flutter analysis finds the flutter speed at 10.9 m s^{-1} where the damping is zero.

The response of the system lower than the flutter speed is not of interest since the oscillations die out with time due to the positive damping (negative maximum λ). An example is presented in Figure 4.2, where the oscillations die out as indicated by positive damping in Figure 4.1. The nonlinearity under flutter speed does not affect system stability since the proposed nonlinearity is of polynomial type and vanishing oscillations mean the higher-order nonlinear contributions would be smaller than linear damping.
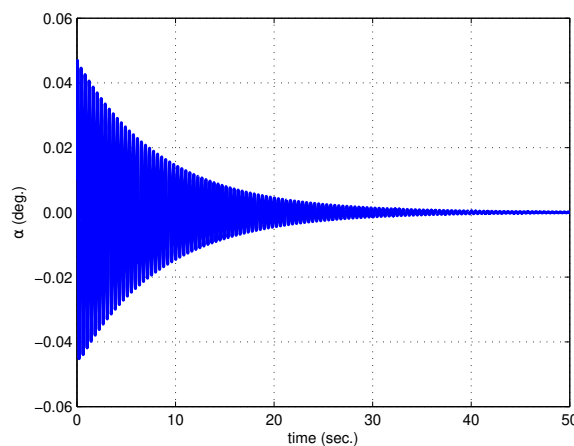

Figure 4.2: Convergent pitch response to perturbation at 5 m s^{-1}.

On the other hand, post-flutter behaviour would be more interesting since the higher-order restoring forces can alter the linear divergent behaviour. Two air-stream values above flutter speed were selected at $U = 1.25U_f$ and $U = 1.40U_f$. For both cases first, the pitch responses were presented in Figure 4.3 and Figure 4.5 to show the divergent behaviour after the flutter. Then the pitch response of the nonlinear system is presented in Figure 4.4 and Figure 4.6 respectively, along with the corresponding non-dimensional phase plane plots, which indicate the topological properties of the state space. The initial conditions of the systems in the phase plane plots are marked with a solid dot. It should be noted that the plots involve only pitching motion; the intersections observed in the phase-plane plots (which do not happen when the full model in four dimensions is considered) are due to the projection of the variable and its time derivative on a 2D plane.
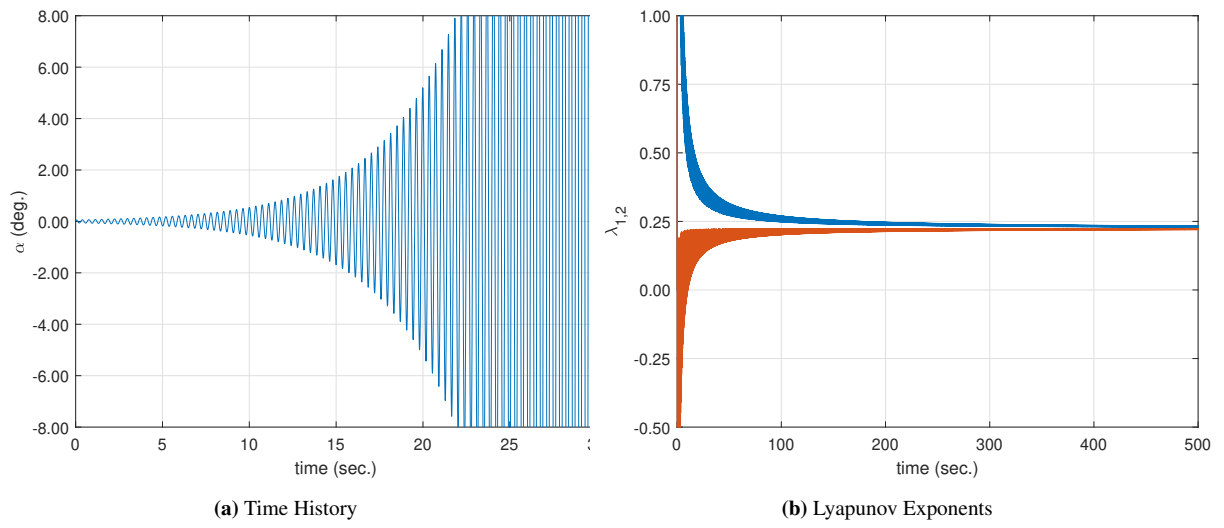
(a) Time History

(b) Lyapunov Exponents

Figure 4.3: Time history, and LCEs for the linear problem after a perturbation at $U = 1.25U_f$

(a) Time-history (transient response)

(b) Time-history (steady-state)

(c) Phase-plane
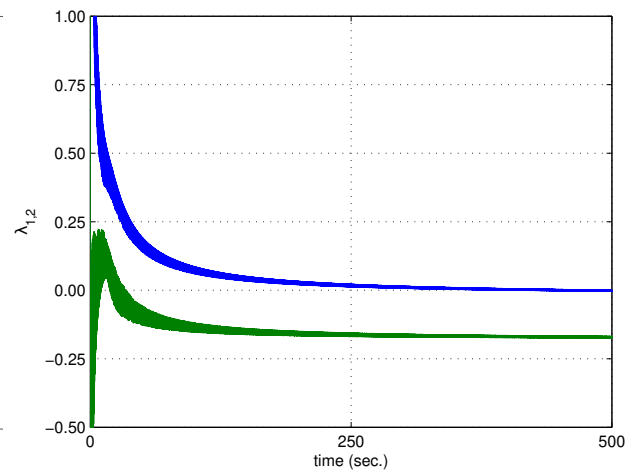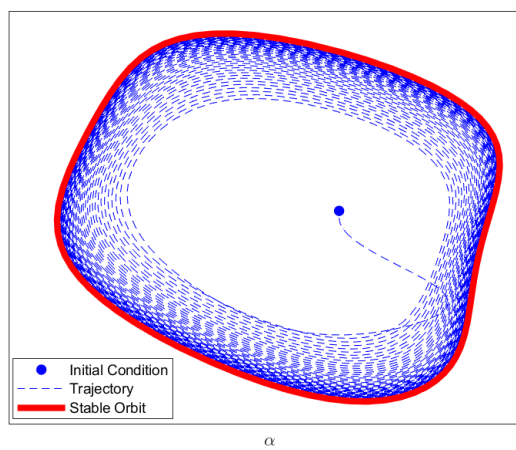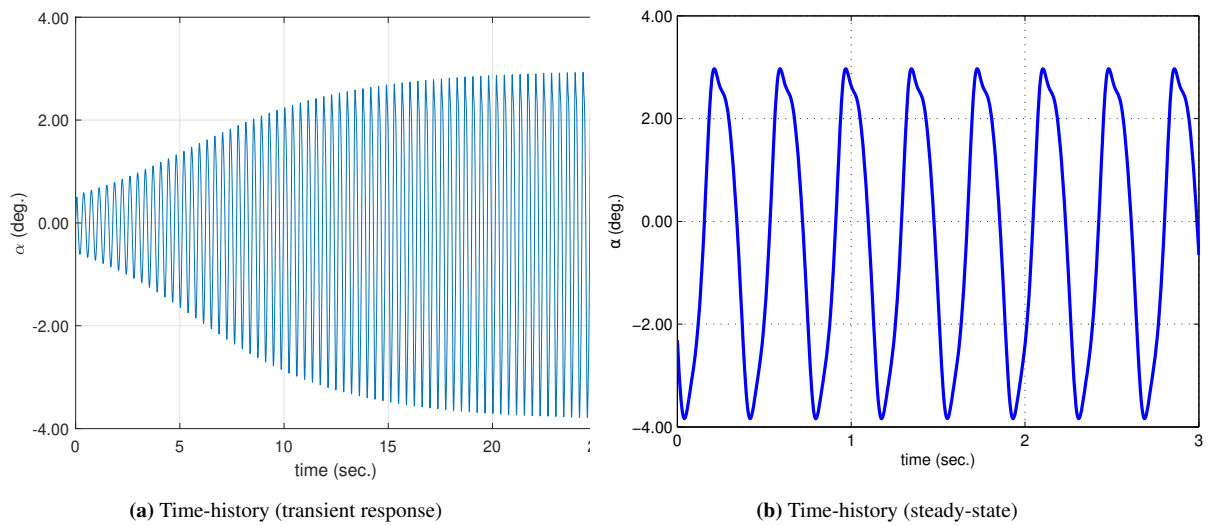

(d) Lyapunov Exponents

Figure 4.4: Time history, phase plane and LCEs for the nonlinear problem after a perturbation at $U = 1.25U_f$

(a) Time History

(b) Lyapunov Exponents
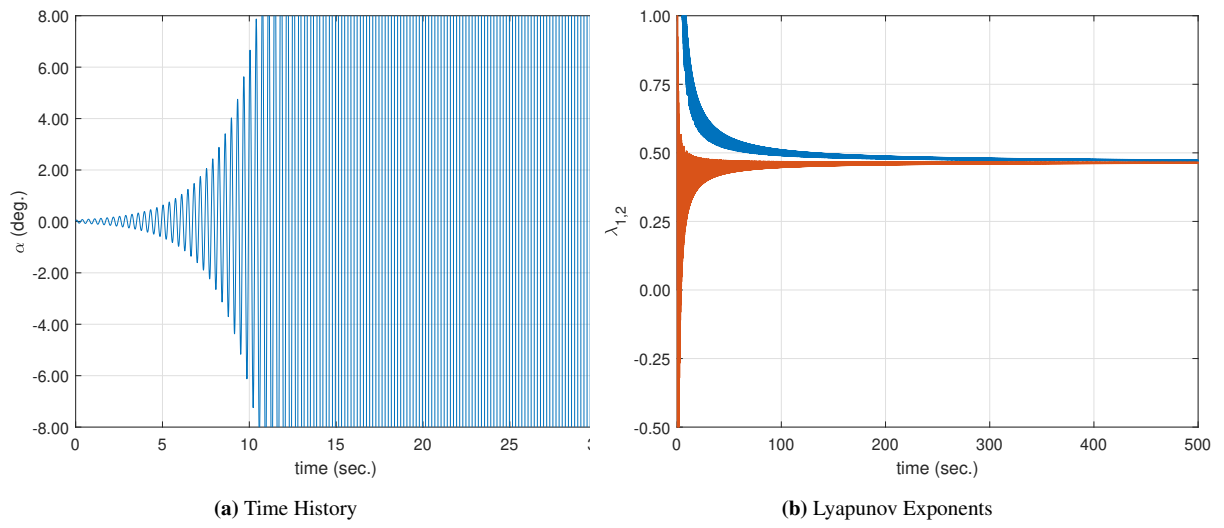
Figure 4.5: Time history, and LCEs for the linear problem after a perturbation at $U = 1.40U_f$

(a) Time-history (transient response)

(b) Time-history (steady-state)

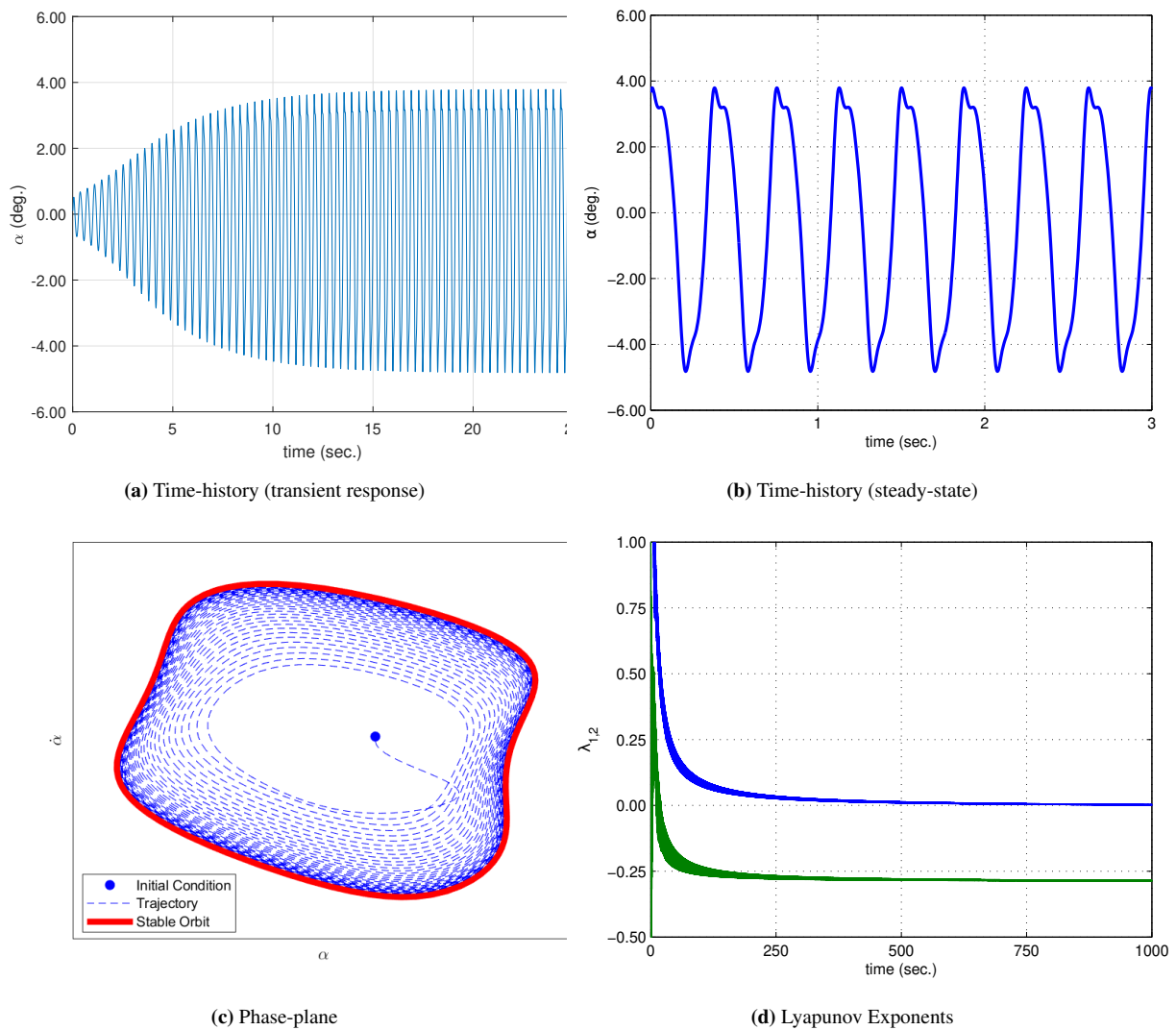**(c)** Phase-plane

(d) Lyapunov Exponents

Figure 4.6: Time history, phase plane and LCEs for the nonlinear problem after a perturbation at $U = 1.40U_f$

When the airstream speed exceeds the flutter speed for a linear system, any perturbation from its equilibrium condition would lead to a divergent response as presented in Figure 4.3 and Figure 4.5. Their LCE estimates are also positive confirming the observed behaviour. However, this did not happen in the presence of a cubic nonlinear restoring force. As a consequence of nonlinearity in stiffness, the system experiences periodic motion (Figure 4.4b and Figure 4.6b) after the transients (Figure 4.4a and Figure 4.6a) die out. The phase portraits converge to an orbit regardless of the initial condition, thus an LCO occurs, as illustrated in Figure 4.4c and Figure 4.6c for flight speeds significantly higher than flutter speed. The amplitude and phase portraits of the responses are in agreement with those of Ref. [22].

From a nonlinear aeroelasticity perspective and within the scope of this work, the periodic orbits of Figure 4.4c and Figure 4.6c are of particular interest. When a nonlinear system has a periodic attractor (for example LCO), zero-valued largest LCE estimates (or converging to zero from a numerical estimation point of view) are expected [30]. This can be observed in Figure 4.4d and Figure 4.6d, which present the time evolution of LCEs for the corresponding flight speed values of $U = 1.25U_f$ and $U = 1.40U_f$. The largest LCE branch converges to zero, while the other tends to be a negative value. Thus, the LCE estimates are compatible with the periodic motion of the system shown in Figure 4.4b and Figure 4.6b. Therefore, the use of LCEs in predicting the nonlinear post-flutter airfoil motion was successfully demonstrated. It is also worth noting that using LCEs as stability indicators can provide two additional benefits. First, LCEs allow us to track the change in the other mode with more damping, which is not possible to extract from time responses. In this particular example, the converging mode damping increased 50% (λ increased from 0.2 at $1.25U_f$ to 0.30 at $1.40U_f$). The second benefit comes from tracking the lowest damping mode for a larger flight speed range. If LCE estimations are extended to cover from zero flight speed to $1.40U_f$, Figure 4.7 is obtained that presents the stability indicators for linear spring (real part of the eigenvalue) and cubic spring (LCEs) cases. Since LCEs are a generalization of linear stability using eigenvalues, it is possible to compare both linear and nonlinear cases. This allows us to understand the impact of nonlinearity before and after the flutter speed. In Figure 4.7 for example, it can be observed that under flutter speed the linear and nonlinear systems have almost equal damping, indicating that the nonlinearities can be neglected. On the other hand, above the flutter speed, the linear system loses stability indicated by the positive real part of the eigenvalues. However, the nonlinear system remains at zero damping ($\lambda = 0$), resulting in an isolated periodic orbit (LCO) rather than a divergent behaviour, showing a completely distinct behaviour as compared to the linear system.
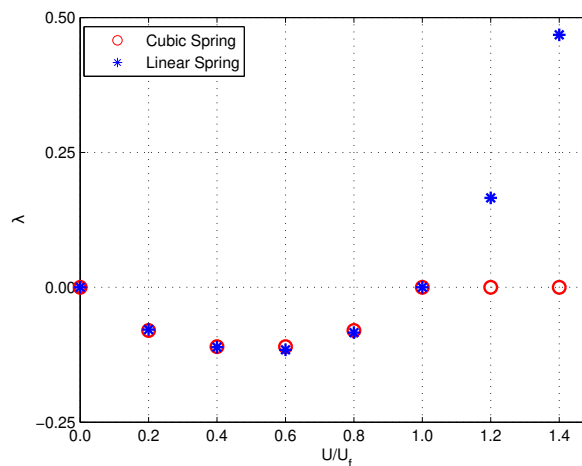

Figure 4.7: Comparison of stability indicators of the linear model and nonlinear model with cubic stiffness.

5. Conclusions

Quantitative stability prediction for aeroelastic problems possessing nonlinear restoring force was presented. The spectrum of the nonlinear aeroelastic systems was estimated using Lyapunov Characteristic Exponents to show that i) nonlinearities can stabilize an otherwise chaotic or divergent system; and ii) the nonlinear behaviour can be identified using LCEs. The Discrete QR decomposition method was used for the practical estimation of Lyapunov Characteristic Exponents. The LCEs are compatible with the real part of the eigenvalues of Linear Time Invariant and Linear Time Periodic problems. Therefore, LCEs are considered to be a natural generalization of stability indicators that are used in conventional engineering practice, including nonlinear aeroelastic stability problems.

A two-dimensional wind tunnel wing model was used to demonstrate the use of LCEs in estimating the nonlinear stability of aeroelastic problems. A cubic restoring force is defined on the spring supporting pitching motion. The behaviours indicated by the resulting LCEs were verified with time marching simulations. The results were compared with the linear model in the post-flutter region. It was shown that the use of LCEs can provide several advantages such as quantitatively tracking the change of stability indicators and comparing the system damping with a linear model, as LCEs are a generalization of the eigenvalue solution for nonlinear problems. Therefore the chaotic and divergent phenomena could better be identified and prevented in the design of aeroelastic systems.

Finally, it should be noted that practical aeroelastic analysis usually involves more complex models. The proposed method can directly be applied directly to high-fidelity models but the convergence of the exponents in a high-fidelity nonlinear model will be computationally demanding, hence limiting the practicality of the method. In this case, the proposed method can be applied to reduced-order models of complex systems. This requires the identification of nonlinear properties, therefore nonlinear model reduction techniques should be implemented before starting the quantitative stability analysis.

Nomenclature

a	position of elastic axis
b	semi-chord
c	viscous damping acting on pitching and plunging
c_i	i=1:6, Unsteady aerodynamic constants
$\mathbf{f}_{nl}$	Nonlinear force due to cubic spring
k	spring stiffness acting on pitching and plunging
m_w	wing mass
m_T	total mass
s	span
w	plunging degree of freedom
$\mathbf{A}$	State space matrix
$\mathbf{C}$	Damping matrix
I_α	Moment of inertia about elastic axis
$\mathbf{H}$	Monodromy matrix
LCE	Lyapunov Characteristic Exponents
$\mathbf{K}$	Stiffness matrix
$\mathbf{M}$	Mass matrix
U	Flight Speed
U_f	Flutter Speed
$\mathbf{Y}$	State transition matrix
α	pitching degree of freedom
ξ	Augmented State of unsteady flow
λ	Converged value of LCEs
ρ	air density

Article Information

References

[1] R. L. Bisplinghoff, H. Ashley, R. L. Halfman, *Aeroelasticity*, Dover, New York, 1996.

[2] S. H. Strogatz, *Nonlinear Dynamics and Chaos: With Applications to Physics, Biology, Chemistry, and Engineering*, Perseus Books, Reading, Massachusetts, 1994.

[3] E. Dowell, J. Edwards, T. Strganac, *Nonlinear aeroelasticity*, J. Aircraft, **40**(5)(2003), 857-874.

[4] B.H.K. Lee, S.J. Price, Y.S. Wong, *Nonlinear aeroelastic analysis of airfoils: bifurcation and chaos*, Prog. Aero. Sci., **35**(3)(1999), 205-334.

[5] X. Jinwu, Y. Yongju, L. Daochun, *Recent advance in nonlinear aeroelastic analysis and control of the aircraft*, Chin J. Aeronaut., **27**(1)(2014),12-22.

[6] L. Adrianova, *Introduction to Linear Systems of Differential Equations*, Translations of Mathematical Monographs, American Mathematical Society, Providence, Rhode Island, 1995.

[7] G. Benettin, L. Galgani, A. Giorgilli, J. Strelcyn, *Lyapunov characteristic exponents for smooth dynamical systems and for Hamiltonian systems; a method for computing all of them part 1: Theory*, Meccanica, **15**(1)(1980), 9-20.

[8] L. Dieci, *Jacobian free computation of Lyapunov exponents.* J. Dynam. Differential Equations, **14**(3)(2002), 697-717.

[9] A. Wolf, J. B. Swift, H. L. Swinney, J. A. Vastano, *Determining Lyapunov exponents from a time series*, Phys. D., **16**(3)(1985), 285–317.

[10] S. J. Price, H. A. Ghanbari, B. H. K. Lee. *The aeroelastic response of a two dimensional airfoil with bilinear and cubic structural nonlinearities*, J. Fluids Struct., **9**(1995), 175–193.

[11] H. Dai, X. Yue, D. Xie, S. N. Atluri, *Chaos and chaotic transients in an aeroelastic system*, J. Sound Vib., **333**(2014), 7267–7285.

[12] L. Librescu, G. Chiocchia, P. Marzocca, *Implications of cubic physical/aerodynamic non-linearities on the character of the flutter instability boundary*, Int. J. Non Linear Mech., **38**(2)(2003), 173–199.

[13] A. Tamer, P. Masarati, *Stability of nonlinear, time-dependent rotorcraft systems using Lyapunov characteristic exponents*, J. Am. Helicop. Soc., **61**(2)(2016), 14-23.

[14] P. Masarati, A. Tamer, *Sensitivity of trajectory stability estimated by Lyapunov characteristic exponents*, Aerosp. Sci. Technol., **47**(2015), 501-510.

[15] N. D. Cong, H. Nam, *Lyapunov's inequality for linear differential algebraic equation*, Acta Math. Vietnam, **28**(1)(2003), 73–88.

[16] A. Tamer, P. Masarati, *Generalized quantitative stability analysis of time-dependent comprehensive rotorcraft systems*, Aerospace, **9**(1)(2022), 10.

[17] P. Masarati, *Estimation of Lyapunov exponents from multibody dynamics in differential-algebraic form*, Proceedings of the Institution of Mechanical Engineers, Part K: Journal of Multi-body Dynamics, **227**(1)(2013), 23-33.

[18] G. Dimitriadis, *Introduction to Nonlinear Aeroelasticity*, Aerospace, Wiley, Chichester, West Sussex, U.K., 2017.

[19] A. Tamer, *Aeroelastic response of aircraft wings to external store separation using flexible multibody dynamics*, Machines, **9**(3)(2021), 61.

[20] B. H. K. Lee, L.Y. Jiang, Y. S. Wong, *Flutter of an airfoil with a cubic restoring force*, J. Fluids Struct., **13**(1999), 75–101.

[21] D. Li, S. Guo, J. Xiang, *Aeroelastic dynamic response and control of an airfoil section with control surface nonlinearities*, J. Sound Vib., **329**(2010), 4756–4771.

[22] A. Abdelkefi, R. Vasconcellos, A. H. Nayfeh, M. R. Hajj, *An analytical and experimental investigation into limit-cycle oscillations of an aeroelastic system*, Nonlinear Dyn., **71**(2013), 159-173.

[23] B.H.K. Lee, L. Liu, K.W. Chung. *Airfoil motion in subsonic flow with strong cubic nonlinear restoring forces*, J. Sound Vib., **281**(2005), 699–717.

[24] K. Geist, U. Parlitz, W. Lauterborn, *Comparison of different methods for computing Lyapunov exponents*, PTEP. Prog. of Theor. Phys, **83**(5)(1990), 875–893.

[25] P. Masarati, A. Tamer, *The real schur decomposition estimates Lyapunov characteristic exponents with multiplicity greater than one*, Proceedings of the Institution of Mechanical Engineers, Part K: Journal of Multi-body Dynamics, **230**(4)(2016), 568–578.

[26] D. Hodges, G. A. Pierce, *Introduction to Structural Dynamics and Aeroelasticity*, Cambridge University Press, Cambridge, England, 2002.

[27] J. R. Wright, J. E. Cooper, *Introduction to Aircraft Aeroelasticity and Loads*, John Wiley & Sons, 2007.

[28] W.A. Silva, R.E. Bartels, *Development of reduced-order models for aeroelastic analysis and flutter prediction using the cfl3dv6.0 code*, J. Fluids Struct., **19**(6)(2004), 729-745.

[29] J. W. Edwards, H. Ashley, J. V. Breakwell, *Unsteady aerodynamic modeling for arbitrary motions*, AIAA Journal, **17**(4)(1979), 365-374.

[30] A. Medio, M. Lines, *Nonlinear Dynamics — A Primer*, Cambridge University Press, 2001.